Increased Nonlinear Coupling between Turbulence and Low-Frequency Fluctuations at the L-H Transition

R. A. Moyer,[1] G. R. Tynan,[1] C. Holland,[1,2] and M. J. Burin[1]

[1]*Mechanical and Aerospace Engineering Department, University of California, San Diego, 9500 Gilman Drive, La Jolla, California 92093*

[2]*Department of Physics, University of California, San Diego, 9500 Gilman Drive, La Jolla, California 92093*

(Received 13 December 2000; published 4 September 2001)

The nonlinear coupling between small scale high-frequency turbulence and larger scale lower-frequency fluctuations increases transiently in transitions to improved confinement in the DIII-D tokamak. This increase starts *before* the rapid turbulence suppression and $E \times B$ shear-flow development in the region that becomes the H-mode transport barrier/shear flow region. After the transition, the coupling returns to L-mode levels. These results are consistent with expectations for spontaneous transitions to improved confinement triggered by a turbulence-driven sheared flow.

DOI: 10.1103/PhysRevLett.87.135001 PACS numbers: 52.35.Ra, 47.27.–i, 52.55.Fa, 92.10.Ty

The confinement of hot dense plasmas in toroidal magnetic configurations is often limited by particle and heat transport due to plasma microturbulence [1]. Under suitable conditions, however, these plasmas undergo spontaneous transitions from low to high confinement states by the formation of radially localized transport barriers in the plasma edge [2] and core [3]. These transport barriers result from the spontaneous formation of a sheared flow [4] which increases the decorrelation rate of turbulent eddies via eddy stretching in the direction of the flow [5]. This suppression of turbulent transport via sheared flow is nearly universal in plasmas, and also occurs in hydrodynamics under suitable conditions described in Ref. [5].

The origin of these spontaneously generated shear flows in plasmas is a critical question. In the initial theoretical work [6], the origin was unspecified. In more recent work the sheared flow was proposed to evolve out of the turbulence in a self-organization process [7–13] driven by the turbulent Reynolds stress [14] which transports and concentrates turbulent momentum in a velocity shear layer. The process is analogous to the generation of zonal flows in the other 2D fluid systems such as the jet streams on Earth, the banding of Jupiter's atmosphere, and the differential rotation of the Sun [15–18]. Viewed as a mode-coupling problem, the kinetic energy associated with the turbulent velocity fluctuations of the fluid is transferred to larger spatial scales via three-wave interactions [19,20].

In this paper we present qualitative evidence that such self-organization takes place using the nonlinear signal processing technique known as bispectral analysis. Three-wave interactions between small scale high-frequency turbulence and larger scale lower-frequency fluctuations increase transiently *prior to* and *during* the transition from low to high confinement (L-H transition) in the region where the shear layer forms. This increase is initially limited to coupling between small ($k_\theta > 2\ \mathrm{cm}^{-1}$) and intermediate-to-large ($k_\theta \approx 0.1\text{–}1\ \mathrm{cm}^{-1}$) scales, and becomes broadband during the transition. After the L-H transition the coupling returns to L-mode values, with residual coupling between small ($k_\theta > 2\ \mathrm{cm}^{-1}$) and large ($k_\theta \approx 0.1\ \mathrm{cm}^{-1}$) scales.

Several workers have studied the electrostatic Reynolds stress $\langle \tilde{v}_r \tilde{v}_\theta \rangle$ using Langmuir probes in the edge of Ohmic and auxiliary heated plasma discharges [21] or during improved Ohmic confinement tokamak discharges [22]. However, due to the high heat loads on probes, results have not been reported during spontaneous L-H transitions in auxiliary heated confinement experiments. Further, probes cannot measure in the plasma core, where self-generated shear (zonal) flows are predicted to modulate the turbulence level and to contribute to the spontaneous formation of internal transport barriers [23]. Direct measurement of the Reynolds stress is thus quite difficult, and so alternative approaches are needed. Consequently, several authors have reformulated the problem as a three-wave mode-coupling problem [13,19,20], transforming the search for changes in the Reynolds stress and shear flow into a related study of the bispectrum of the potential fluctuations $B_{k_3}(\mathbf{k}_1, \mathbf{k}_2) \equiv \langle \phi(\mathbf{k}_3)\phi(\mathbf{k}_1)\phi(\mathbf{k}_2) \rangle$. The cross power transfer between the turbulent Reynolds stress due to electrostatic $\mathbf{E} \times \mathbf{B}$ fluid velocity fluctuations, $k_{1r}k_{2\theta}\phi(\mathbf{k}_1)\phi(\mathbf{k}_2)$, and the shear flow, $\mathbf{k}_3\phi(\mathbf{k}_3)$, can be related to the above bispectrum if the fluctuating wave numbers are estimated by their mean values [20,24]. An increase in the shear-flow energy due to the Reynolds stress should thus be accompanied by an increase in the bispectrum. A similar conclusion was reached using an energetics formalism in a recent paper by Diamond *et al.* [19].

An increase in the bispectrum can occur via increases in the turbulence or shear-flow amplitudes and/or by an increase in the coherence between different fluctuation scales. Since the turbulence and shear-flow amplitudes do not change significantly prior to the L-H transition (Fig. 1) [25], we look for changes in the three-wave phase coherence across the transition using the (squared) auto-bicoherence $\hat{b}^2_{k_3}(k_1, k_2) \equiv \frac{|B_{k_3}(k_1,k_2)|^2}{\langle|\phi_{k_3}|^2\rangle\langle|\phi_{k_1}\phi_{k_2}|^2\rangle}$ which provides a measure of the significance of phase-coherent three-wave

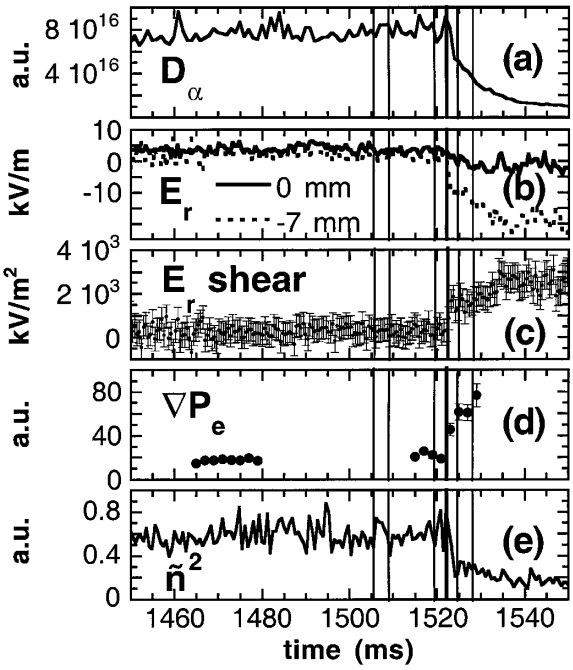

FIG. 1. A L-H transition (thick line) showing (a) D_α drop, (b) E_r at (0 mm) and 7 mm inside (-7 mm) the separatrix, (c) edge E_r shear estimated from the E_r difference in (b), (d) ∇P_e, and (e) density fluctuation power $\tilde{n}^2$ in the edge measured by reflectometry. The thin vertical lines are the bicoherence analysis times in Fig. 2.

interactions with $\mathbf{k}_3 = \mathbf{k}_1 + \mathbf{k}_2$ [20], independent of the fluctuation amplitude.

The $\mathbf{k}$ domain results are transformed into the frequency domain using the frozen-flow hypothesis, which states that, if the fluctuation structure does not change significantly as it convects past the probe (if the propagation time δt through the sampling volume d is short relative to the autocorrelation time τ_{corr}), the frequency can be linearly related to the wave number via the measured phase velocity v_θ. Here, $\delta t = d/v_\theta \sim 5\ \mu\text{s} \ll \tau_{\text{corr}} \sim 15$–$30\ \mu\text{s}$ during the L mode and $\delta t \leq 1\ \mu\text{s} \ll \tau_{\text{corr}} \approx 5$–$15\ \mu\text{s}$ during the H mode. The measured $k_\theta \propto f$; in L mode, for example, $k_\theta = 0.1\ \text{cm}^{-1}$ ($2\ \text{cm}^{-1}$) at $f = 10$ (200) kHz. Since there is no Doppler shift for the shear flow (because it has $k_\theta \sim 0$) the low-frequency ($f \sim 0$) nature of the sheared flow is retained. Therefore we expect coupling between small scale turbulence and large scale shear flows to be manifested as simultaneous coupling among triads of frequencies $f_1 \approx f_2$ approximately hundreds of kHz and the corresponding difference frequencies $f_3 \ll f_1, f_2 \approx 0$ kHz.

The data presented here were acquired in reproducible neutral beam heated discharges with spontaneous L-H transitions in the DIII-D tokamak. The plasma undergoes a L-H transition at 1522.6 ms as indicated by a drop in the edge D_α emission (a measure of the plasma efflux) [Fig. 1(a)]. The radial electric field E_r, measured by charge exchange recombination (CER) spectroscopy [26], increases in a narrow layer just inside the separatrix [Fig. 1(b)], where for clarity we plot only the two chords that bracket the radius of the probe measurements. This E_r shear layer [Fig. 1(c)] induces a sheared rotation on the edge fluctuations, which subsequently undergo an amplitude reduction at the transition as indicated by the density fluctuation power $\tilde{n}^2$ measured just inside the shear layer by reflectometry [Fig. 1(e)]. A radially localized "transport barrier" is formed, as indicated by the increase in the electron pressure gradient ∇P_e in the edge after the transition [Fig. 1(d)]. A detailed discussion of the L-H transition phenomenology has be presented elsewhere [3,25].

The turbulence data were obtained with a reciprocating Langmuir probe on the outboard midplane of the torus [27] measuring ion saturation current I_{sat} and poloidally separated floating potentials V_{float}, during the stationary maximum insertion point (the "dwell"). The dwell radius was varied on repeat discharges to obtain the radial profile of the turbulence measurements across the L-H transition. The squared auto-bicoherence $\hat{b}^2_{f_3}(f_1, f_2)$ was computed from V_{float} and I_{sat} data in 3.48 ms intervals at the times indicated in Fig. 1 using established techniques [28]. Each interval was analyzed with 34 realizations of 512 samples at a frequency of 5 Msamples/s. We first consider the summed auto-bicoherence, defined as $b^2(f_3) \equiv \sum_{f_1+f_2=f_3} \hat{b}^2_{f_3}(f_1, f_2)$, which provides an indication of the relative amount of coherent three-wave coupling at frequency f_3 to all other frequencies, such that $f_3 = f_1 \pm f_2$. The noise floor of $b^2(f_3)$ is estimated following the established literature as $1/N \sim 0.03$, where N equals the number of realizations, well below the calculated values of $b^2(f_3)$. This estimate is in good agreement with $b^2(f_3)$ calculated from a random signal which contained no coupling. Although the absolute value of our bicoherence estimator has probably not converged due to the short record lengths available [29], identical record lengths and the number of realizations allow us to estimate the time dependence of gross features in the bicoherence. The use of V_{float} and I_{sat} in place of plasma potential and density, respectively, neglects T_e fluctuations with well-known limitations (see Appendix B of [25]). However, we expect the gross features of the bicoherence to be similar for all fluctuating fields (as we show for V_{float} and I_{sat}).

Just before the L-H transition (-2.5 ms), the potential fluctuation power begins to decrease [Fig. 2(a)] coincident with a large increase in $b^2(f_3)$ of the potential fluctuations across the entire frequency range [Fig. 2(b)]. Just after the transition ($+2.6$ ms), the fluctuations are strongly suppressed [Fig. 2(a)], and $b^2(f_3)$ decreases toward L-mode levels, except in the ranges $f_3 < 30$ kHz and $200 < f_3 < 400$ kHz. By 6 ms after the transition, $b^2(f_3)$ has returned to the initial L-mode values for all f_3. Similar results are obtained for I_{sat} [Fig. 2(c)], except that, even 6 ms after the transition, increased coupling persists for $f_3 < 60$ kHz and $100 < f_3 < 400$ kHz.

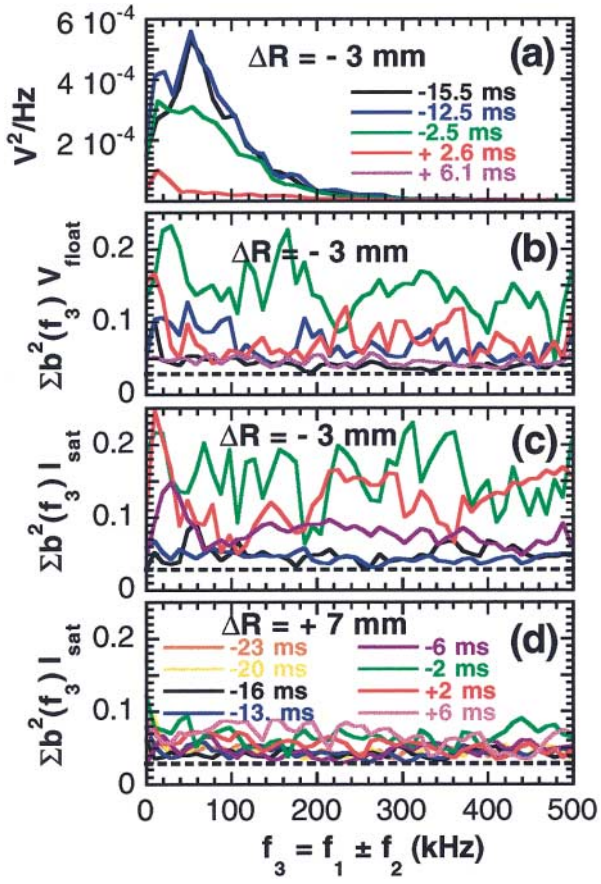

FIG. 2 (color). (a) Potential fluctuation autopower spectra and summed bicoherence $b^2(f_3)$ for (b) V_{float}, and (c) I_{sat} 3 mm inside the separatrix at times relative to the L-H transition time. (d) This panel shows $b^2(f_3)$ for I_{sat} 7 mm outside the separtrix in a similar discharge with times as indicated. The dashed lines in (b), (c), and (d) indicate the statistical significance level.

The structure of the three-wave coupling is indicated by the squared auto-bicoherence in frequency space $\hat{b}^2_{f_3}(f_1, f_2)$ [Fig. 3]. At each (f_1, f_2) the degree of phase coherence for triad interactions with $f_3 = f_1 \pm f_2$ is plotted; the $f_2 > 0$ triangle corresponds to sum coupling $f_3 = f_1 + f_2$, and is bounded on the left at $f_1 = f_2$ by symmetry and on the right by $f_3 = f_N$ since frequencies above f_N are not measured. The $f_2 < 0$ region corresponds to difference coupling $f_3 = f_1 - f_2$ and is bounded on the left at $f_1 = -f_2$ by symmetry and on the right by $f_3 = 0$. In early L mode [Fig. 3(a)], there is little structure to the three-wave coupling. Just before the transition [Fig. 3(b)], significant coupling develops between pairs of high (400–1000 kHz) and low-to-intermediate difference frequencies (20–200 kHz). Just after the L-H transition [Fig. 3(c)], this coupling shifts to nearly equal high and smaller difference frequencies ($f_1 \sim f_2 \sim 300$–1200 kHz; $f_3 < 60$ kHz) in the presence of broadband coupling that may result from an increase in the "burstiness" of the signal. By 6 ms after the transition, ∇P_e is 3 times larger [Fig. 1(d)], the

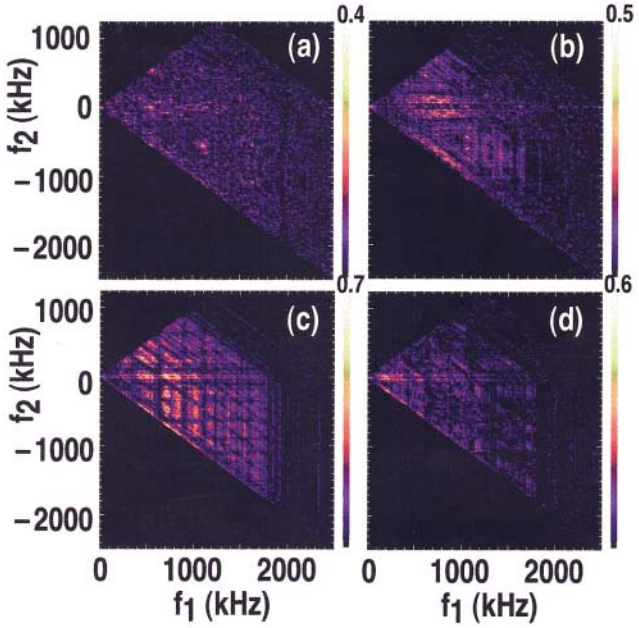

FIG. 3 (color). Auto-bicoherence $\hat{b}^2_{k_z}(k_1, k_2)$ of the ion saturation current 3 mm inside the separatrix (a) 15.5 ms before, (b) 2.5 ms before, (c) 2.5 ms after, and (d) 6.1 ms after the L-H transition.

broadband coupling has disappeared, and only coupling between nearly equal high and low difference frequencies remains ($f_1 \sim f_2 \sim 100$–1000 kHz; $f_3 < 50$ kHz) [Fig. 3(d)]. This coupling eventually disappears more than 10 ms after the transition.

Bispectral analysis of data 7 mm outside the separatrix [Fig. 2(d)] shows no such temporal variation, indicating that the bicoherence where measured changes only in the region of the strong shear flow. The time dependence of the total bicoherence $b^2 = \sum_{f_1} \sum_{f2} b^2_{f3}(f_1, f_2)$ (a measure of the relative strength of nonlinear coupling integrated over all scales) is shown in Fig. 4 inside (-3 mm) and outside ($+7$ mm) the separatrix, and indicates the temporal and spatial localizations of the changes relative to the L-H transition.

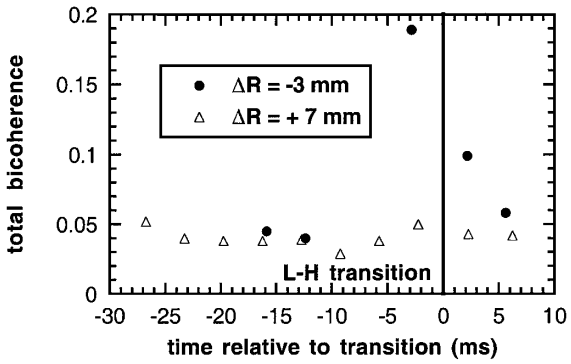

FIG. 4. Evolution of the total bicoherence of I_{sat} 3 mm inside (•) and 7 mm outside (△) the separatrix.

These results indicate that three-wave coupling between low and high frequencies (large and small scales) increases just before and during the *L-H* transition. This transient increase (i) starts *before* the turbulence reduction and rapid increase in $\mathbf{E} \times \mathbf{B}$ shear flow, (ii) occurs in the region of increased velocity shear, and (iii) decays within a few milliseconds after the *L-H* transition. These results are consistent with expectations for a transient Reynolds stress-driven zonal flow triggering the *L-H* transition [30,31]. In these models, as the Reynolds stress decays, the increased pressure gradient [Fig. 1(d)] sustains a mean (diamagnetic) shear flow distinct from the initial Reynolds stress shear flow in the steady-state *H* mode.

Several questions about these results remain. First, the transient nature of the *L-H* transition limits the bispectral analysis here to a small number of realizations, so that the values are probably not completely converged [29]. However, experience with strongly correlated test signals using similar numbers of realizations gives reasonable agreement with analytically calculated values, in terms of both magnitude and location in the f_1-f_2 plane. We therefore suggest that what is important here is the transient appearance of the coupling between large and small scales, rather than the actual strength of that coupling.

Second, are the low-frequency fluctuations in fact the zonal flows suggested by theory and computation? Zonal flows should have $f \sim 0$ with finite spectral width δf determined by collisional damping of the zonal flow [32]. In the DIII-D core, $\delta f \approx 5$ kHz, significantly lower than the difference frequencies reported here. This estimate assumes that the fluctuations are small and that ion-ion collisions dominate the zonal flow damping. These assumptions break down in the edge where the fluctuations are large and ion-neutral collisions may dominate the damping rate. Unfortunately, no estimates have been published for zonal-flow damping in the edge, and we cannot determine if the difference frequencies seen here are consistent with a Reynolds stress-driven flow in the edge.

Third, one would also like to measure the rate of energy transfer from smaller to larger spatial scales. The data requirements [33] for this calculation are prohibitive for DIII-D, and so this issue must be addressed on other devices.

Finally, the bicoherence observations shown here suggest that similar signatures could be observed in density fluctuations during internal transport barrier formation.

The authors thank R. J. Groebner (CER) and E. J. Doyle (reflectrometry) for providing the data in Fig. 1, and acknowledge useful discussions with P. Diamond, T. L. Rhodes, and S. Krasheninnikov. This work was supported by the U.S. Department of Energy under Grants No. DE-FG03-95ER–54294 and No. DE-FG03-99ER54553. C. H. performed this research under an appointment to the Fusion Energy Sciences Fellowship Program, administered by Oak Ridge Institute for Science and Education under a contract between the U.S. Department of Energy and the Oak Ridge Associated Universities.

[1] B. A. Carreras, IEEE Trans. Plasma Sci. **25**, 1281 (1997).
[2] F. Wagner *et al.,* Phys. Rev. Lett. **49**, 1408 (1982).
[3] K. H. Burrell, Phys. Plasmas **6**, 4418 (1999).
[4] R. J. Groebner, K. H. Burrell, and R. P. Seraydarian, Phys. Rev. Lett. **64**, 3015 (1990).
[5] P. W. Terry, Rev. Mod. Phys. **72**, 109 (2000).
[6] H. Biglari, P. H. Diamond, and P. W. Terry, Phys. Fluids B **4**, 1385 (1990).
[7] A. Hasegawa and M. Wakatani, Phys. Rev. Lett. **59**, 431 (1987).
[8] W. Horton and A. Hasegawa, Chaos **4**, 227 (1994).
[9] Z. Lin *et al.,* Science **281**, 1835 (1998).
[10] M. Beer *et al.,* Plasma Phys. Controlled Fusion **35**, 973 (1993).
[11] A. Dimits *et al.,* Phys. Rev. Lett. **77**, 71 (1996).
[12] R. D. Sydora *et al.,* Plasma Phys. Controlled Fusion **38**, A281 (1996).
[13] P. H. Diamond *et al.,* in Proceedings of the 18th IAEA Fusion Energy Conference, Sorrento, Italy, 2000 (to be published).
[14] P. H. Diamond and Y.-B. Kim, Phys. Fluids **3**, 1626 (1991).
[15] F. H. Busse, Chaos **4**, 123 (1994).
[16] F. De Rooij, P. F. Linden, and S. B. Dalziel, J. Fluid Mech. **383**, 249 (1999).
[17] E. R. Weeks *et al.,* Science **278**, 1598 (1997).
[18] P. S. Marcus, T. Kundu, and C. Lee, Phys. Plasmas **7**, 1630 (2000).
[19] P. H. Diamond *et al.,* Phys. Rev. Lett. **84**, 4842 (2000).
[20] G. R. Tynan *et al.,* Phys. Plasmas **8**, 2691 (2001).
[21] C. Hidalgo *et al.,* Phys. Rev. Lett. **83**, 2203 (1999).
[22] Y. H. Xu *et al.,* Phys. Rev. Lett. **84**, 3867 (2000).
[23] Z. Lin *et al.,* Phys. Rev. Lett. **83**, 3645 (1999).
[24] K. S. Lii, M. Rosenblatt, and C. Van Atta, J. Fluid Mech. **77**, 45 (1976).
[25] R. A. Moyer *et al.,* Phys. Plasmas **2**, 2397 (1995).
[26] P. Gohil, K. H. Burrell, and T. N. Carlstrom, Nucl. Fusion **38**, 93 (1988).
[27] J. G. Watkins *et al.,* Rev. Sci. Instrum. **63**, 4728 (1992).
[28] Y. C. Kim and E. J. Powers, IEEE Trans. Plasma Sci. **PS-7**, 120 (1979).
[29] D. Gresillon and M. S. Mohamed-Benkadda, Phys. Fluids **31**, 1904 (1988).
[30] B. A. Carreras *et al.,* Phys. Plasmas **1**, 4014 (1994).
[31] B. N. Rogers, J. F. Drake, and A. Zeiler, Phys. Rev. Lett. **81**, 4396 (1998).
[32] T. S. Hahm *et al.,* Plasma Phys. Controlled Fusion (Suppl. 5A) **42**, A205 (1999).
[33] Y. Kim *et al.,* Phys. Plasmas **3**, 3998 (1996).